

# Moveout-based geometrical-spreading correction for converted waves

Xiaoxia Xu<sup>1</sup> and Ilya Tsvankin<sup>2</sup>

<sup>1</sup>Formerly Colorado School of Mines, Department of Geophysics, Center for Wave Phenomena; presently ExxonMobil Upstream Research Company, Houston, TX 77252.

<sup>2</sup>Colorado School of Mines, Department of Geophysics, Center for Wave Phenomena, Golden, CO 80401-1887.

## ABSTRACT

Geometrical-spreading correction is an important component of amplitude-variation-with-offset (AVO) analysis, which provides high-resolution information for anisotropic parameter estimation and fracture characterization. Here, we extend the algorithm of moveout-based anisotropic spreading correction (MASC) to mode-converted PSV-waves in VTI (transversely isotropic with a vertical symmetry axis) media and symmetry planes of orthorhombic media.

While the geometrical-spreading equation in terms of reflection traveltimes has the same form for all wave modes in laterally homogeneous media, reflection moveout of PS-waves is more complicated than that of P-waves (e.g., it can become asymmetric in common-midpoint geometry). Still, for models with a horizontal symmetry plane, long-spread reflection traveltimes of PS-waves can be well-approximated by the Tsvankin-Thomsen and Alkhalifah-Tsvankin moveout equations, which are widely used for P-waves. Although the accuracy of the Alkhalifah-Tsvankin equation is somewhat lower, it includes less moveout parameters and helps to maintain the uniformity of the MASC algorithm for P- and PS-waves. The parameters of both moveout equations are obtained by least-squares traveltimes fitting or semblance analysis and are different from those for P-waves.

Testing on full-wavefield synthetic data generated by the reflectivity method for layered VTI media confirms that MASC accurately reconstructs the plane-wave conversion coefficient from conventional-spread PS data. Errors in the estimated conversion coefficient, which become noticeable at moderate and large offsets, are mostly caused by offset-dependent transmission loss of PS-waves.

**Key words:** Mode conversions, AVO analysis, geometrical spreading, VTI media, azimuthal anisotropy, nonhyperbolic moveout

## Introduction

AVO analysis of P-wave data can provide essential information for anisotropic parameter estimation and fracture characterization and (e.g., Rüger, 2001; Neves et al., 2003). However, inversion of the wide-azimuth P-wave AVO response for the pertinent anisotropy parameters is generally ambiguous even for the simple HTI (transversely isotropic with a horizontal symmetry axis) model formed by a system of vertical, penny-shaped cracks in isotropic host rock (Rüger and Tsvankin, 1997; Rüger, 2001). In principle, the nonuniqueness of AVO

analysis can be overcome by combining the P-wave AVO gradient with the NMO ellipse (Bakulin et al., 2000a), but this approach has serious limitations. First, the NMO ellipse can be reconstructed only for relatively thick reservoirs; second, the difference in vertical resolution between amplitude and traveltimes methods can lead to distorted estimates for heterogeneous reservoir formations (Xu and Tsvankin, 2007).

For surveys with multicomponent acquisition, the AVO response of P-waves can be supplemented with that of mode-converted PS-waves. The main advantage

of combining PP and PS amplitude signatures is that they are determined by rock properties on the same scale near the top or bottom of the reservoir. Bakulin et al. (2000a) showed that the azimuthally varying AVO gradients of PP- and PS-waves reflected from an HTI medium constrain both the normal and tangential compliances of the fractures. The compliances can then be related to such physical properties as fracture density and fluid infill. Although this technique was introduced for boundaries between isotropic and HTI media, it remains valid for the lower-symmetry orthorhombic model that describes a vertical fracture system in a VTI background matrix (Bakulin et al., 2000b). A more general methodology for joint inversion of the long-offset, wide-azimuth AVO responses of PP-waves and split PS-waves in azimuthally anisotropic media was developed by Jilek (2002).

Since shear-wave (and, therefore, converted-wave) amplitudes are highly sensitive to the presence of anisotropy along the raypath, robust estimation of PS-wave reflection (conversion) coefficients is impossible without an accurate geometrical-spreading correction. As discussed by Tsvankin (1995, 2005) and Xu et al. (2005), the geometrical spreading of SV-waves in TI media is controlled primarily by the parameter  $\sigma \equiv (V_{P0}^2/V_{S0}^2)(\epsilon - \delta)$ , which is typically much larger than the Thomsen parameters  $\epsilon$  and  $\delta$  responsible for P-wave amplitudes ( $V_{P0}$  and  $V_{S0}$  are the symmetry-direction P- and S-wave velocities, respectively).

To correct AVO signatures for amplitude distortions in the overburden, it is convenient to represent geometrical spreading through reflection traveltimes. Following paraxial ray theory (Červený, 2001), Xu et al. (2005) obtained geometrical spreading of pure reflection modes (PP or SS) in layered, arbitrarily anisotropic media as a function of traveltime derivatives. Although this equation is strictly valid only for laterally homogeneous models, it remains sufficiently accurate in the presence of moderate dips and mild lateral velocity variation.

By combining this geometrical-spreading formulation with a 3D extension of the Alkhalifah-Tsvankin (1995) nonhyperbolic moveout equation, Xu and Tsvankin (2006a) developed a practical and robust algorithm for moveout-based anisotropic spreading correction (“MASC”). The accuracy of MASC for wide-azimuth, long-spread P-wave data from layered orthorhombic media was confirmed by dynamic ray tracing and full-wavefield synthetic modeling (Xu and Tsvankin, 2006b). The synthetic tests also demonstrate that if the azimuthal variation of geometrical spreading is not negligible, MASC cannot be replaced by empirical gain corrections even in qualitative AVO analysis.

Here, the methodology of MASC is extended to PS-waves converted at the reflector (so-called “C-waves”) in laterally homogeneous, anisotropic media. First, we show that despite the asymmetry of the raypath of

mode conversions, their geometrical spreading is expressed through reflection traveltime in the same way as that for P-waves. Second, by employing the Tsvankin-Thomsen (1994) and Alkhalifah-Tsvankin (1995) moveout equations, the MASC algorithm is adapted for PSV-waves acquired in vertical symmetry planes of layered TI and orthorhombic media. Finally, we conduct a full-wavefield synthetic study to evaluate the accuracy of MASC in estimating the conversion coefficient and compare its performance with that of empirical gain corrections used in practice.

## 1 MOVEOUT-BASED GEOMETRICAL-SPREADING EQUATION FOR PS-WAVES

One of the most significant differences between P- and PS-waves is the asymmetry of the raypath and moveout of mode conversions. If the medium is laterally heterogeneous or anisotropic without a horizontal symmetry plane, the traveltime of PS-waves does not stay the same when the source and receiver are interchanged (Thomsen, 1999; Tsvankin and Grechka, 2000; Dewangan, 2004). Because of this moveout asymmetry, PS-wave reflection traveltime on common-midpoint (CMP) gathers may not be an even function of offset and cannot be described by conventional moveout equations for P-waves. Therefore, the two key components of MASC (i.e., the geometrical-spreading and moveout equations) have to be revisited for converted waves.

The general traveltime-based expression for geometrical spreading of pure modes is derived in Appendix A of Xu et al. (2005). Although the derivation assumes reflection moveout to be symmetric (i.e., independent of the sign of offset), the final result turns out to be valid for converted waves. The ray-theory representation of geometrical spreading at the earth’s surface (Červený, 2001) includes traveltime derivatives with respect to four variables – the horizontal coordinates of the source and receiver. If the medium is laterally homogeneous, the number of independent variables can be reduced to two (offset  $x$  and azimuth  $\alpha$ ), even for arbitrary anisotropic symmetries. For pure reflection modes, the azimuth varies only from  $0^\circ$  to  $180^\circ$  because their traveltime remains the same when the source and receiver are interchanged.

The only modification required to account for the asymmetric moveout of converted waves is extension of the range of azimuths to  $360^\circ$ . Then the definition of azimuth (equation A-3 of Xu et al., 2005) takes the form

$$\alpha = \begin{cases} \tan^{-1} \left[ \frac{x_2^r - x_2^s}{x_1^r - x_1^s} \right] & x_1^r - x_1^s > 0, \\ \tan^{-1} \left[ \frac{x_2^r - x_2^s}{x_1^r - x_1^s} \right] + \pi & x_1^r - x_1^s < 0, \end{cases} \quad (1)$$

where  $x_{1,2}^s$  and  $x_{1,2}^r$  are the horizontal source and receiver coordinates, respectively. Compared to the orig-

inal definition for pure modes, equation 1 contains an additional constant ( $\pi$ ) for  $x_1^r - x_1^s < 0$ , which does not change traveltime derivatives.

Hence, the moveout-based geometrical-spreading equation given by Xu et al. (2005) is entirely valid for converted waves:

$$L(x, \alpha) = (\cos \phi^s \cos \phi^r)^{1/2} \left[ \frac{\partial^2 T}{\partial x^2} \frac{\partial T}{\partial x} \frac{1}{x} + \frac{\partial^2 T}{\partial x^2} \frac{\partial^2 T}{\partial \alpha^2} \frac{1}{x^2} - \left( \frac{\partial T}{\partial \alpha} \right)^2 \frac{1}{x^4} \right]^{-1/2} \quad (2)$$

where  $T$  is the traveltime, and  $\phi^s$  and  $\phi^r$  are the angles between the ray and the vertical at the source and receiver locations, respectively. Equation 2 can be used for any reflected wave (pure or converted) in laterally homogeneous, arbitrarily anisotropic media. Application of this equation to events with asymmetric moveout, however, requires certain care because the traveltime derivatives are different for “reciprocal” source-receiver pairs with azimuths  $\alpha \pm \pi$ .

Note that the only source of moveout asymmetry for converted waves in laterally homogeneous media is the presence of anisotropic layers that do not have a horizontal symmetry plane. Next, we verify that our formalism accurately describes the geometrical spreading of PS-waves in the simplest model of this type, which includes a single homogeneous TI layer with a tilted symmetry axis (TTI; see Figure 1). The TTI parameters used in our test are taken from the physical model of Dewangan et al. (2006).

Figure 1 shows the traveltime surface of the fast PS-wave computed by anisotropic ray tracing. In the symmetry-axis plane (i.e., in the vertical plane that contains the symmetry axis), the fast S-wave represents an SV mode because it has in-plane polarization. Since the horizontal plane in this model is not a plane of symmetry, the traveltime surface in CMP geometry is asymmetric with respect to the global minimum. Also, the minimum traveltime is shifted from the common midpoint to an offset that exceeds 0.5 km.

Since it is difficult to approximate this traveltime surface with a Taylor series, we employed a cubic-spline function. Substituting the traveltime derivatives obtained from this spline function into equation 2, we computed the spreading for the PSV-wave in the symmetry-axis plane. Comparison with dynamic ray tracing in Figure 2 confirms the accuracy of equation 2 for converted waves with asymmetric moveout. Except for the discrepancies at large  $x \rightarrow \pm 3$  km and zero offset, which are caused by numerical difficulties in estimating the second-order time derivatives, the spreading computed by our method is close to that obtained by ray tracing.

Although this test proves that MASC can handle arbitrary moveout functions, the rest of the paper is focused on models with a horizontal symmetry plane, in which PS-wave moveout is symmetric.

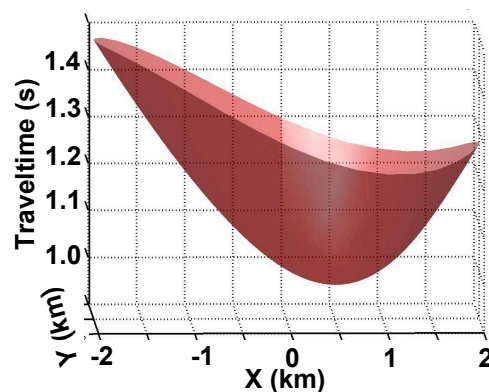


**Figure 1.** Traveltime surface of the fast PS-wave computed for a horizontal TTI layer in CMP geometry. The model parameters are  $V_{P0} = 2.6$  km/s,  $V_{S0} = 1.38$  km/s,  $\epsilon = 0.46$ ,  $\delta = 0.11$ , and  $\gamma = 0$ . The tilt of the symmetry axis from the vertical is  $\nu = 70^\circ$ , the layer’s thickness is 1 km. Note the asymmetry of the surface with respect to the global traveltime minimum, which does not correspond to zero offset.

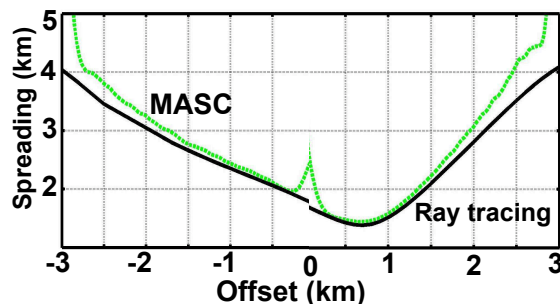


**Figure 2.** Comparison of the geometrical spreading for the PS-wave computed from equation 2 (dashed line) and ray tracing (solid) in the symmetry-axis plane of the model in Figure 1. The “jitters” in the output of MASC correspond to local errors in approximating the traveltime surface.

## 2 MASC ALGORITHM FOR PS-WAVES

Outside of the symmetry planes of azimuthally anisotropic media, a P-wave incident upon a horizontal reflector excites two split PS-waves which have to be separated using polarization analysis. To avoid this complication and facilitate AVO analysis, we assume that the acquisition line is confined to a vertical symmetry plane of the model. Then a P-wave source generates only a P-to-SV conversion polarized in the incidence plane. The goal of this section is to extend the MASC methodology of Xu and Tsvankin (2006a) to PSV-waves recorded in vertical symmetry planes of horizontally layered VTI, HTI, and orthorhombic media.

As is the case for P-waves, the key issue in implementing equation 2 for mode conversions is to find a smooth, relatively simple traveltime approximation that

can be used for a wide range of offsets and azimuths. Long-spread reflection moveout of P-waves in layered VTI media is well-described by the Tsvankin-Thomsen (1994) nonhyperbolic equation:

$$T^2(x) = T_0^2 + A_2 x^2 + \frac{A_4 x^4}{1 + A x^2}, \quad (3)$$

where  $T_0$  is the zero-offset time,  $A_2 = V_{\text{nmo}}^{-2}$  controls hyperbolic moveout ( $V_{\text{nmo}}$  is the normal-moveout velocity), and  $A_4$  is the quartic coefficient responsible for nonhyperbolic moveout at large offsets. The parameter  $A$  depends on the horizontal velocity and is introduced to make  $T(x)$  convergent at  $x \rightarrow \infty$ . With an appropriate substitution of the moveout parameters, equation 3 gives sufficient accuracy for PS-wave traveltimes in horizontally-layered VTI media (Tsvankin, 2005).

By taking into account the azimuthal variation of the moveout parameters  $A_2$ ,  $A_4$ , and  $A$ , Al-Dajani et al. (1998) extended equation 3 to P-waves in orthorhombic media:

$$T^2(x, \alpha) = T_0^2 + A_2(\alpha) x^2 + \frac{A_4(\alpha) x^4}{1 + A(\alpha) x^2}, \quad (4)$$

$$A_2(\alpha) = A_2^{(1)} \sin^2 \alpha + A_2^{(2)} \cos^2 \alpha, \quad (5)$$

$$A_4(\alpha) = A_4^{(1)} \sin^4 \alpha + A_4^{(2)} \cos^4 \alpha + A_4^{(x)} \sin^2 \alpha \cos^2 \alpha. \quad (6)$$

The dependence of  $A_2$  on the azimuth  $\alpha$  is described by the NMO ellipse (Grechka and Tsvankin, 1998), and equation 6 for  $A_4$  is derived by Al-Dajani et al. (1998) for a horizontal orthorhombic layer. Note that HTI can be treated as a special case of the more general orthorhombic model. It is assumed in equations 4–6 that  $\alpha = 0$  corresponds to the symmetry plane  $[x_1, x_3]$ , so  $A_2^{(1,2)}$  and  $A_4^{(1,2)}$  are the symmetry-plane moveout coefficients, while  $A_4^{(x)}$  contributes to nonhyperbolic moveout in off-symmetry directions. Because of the difficulties in treating split PS-waves outside of the symmetry planes, equation 4 has not been applied to mode conversions.

Alkhalifah and Tsvankin (1995) proposed a simpler nonhyperbolic moveout equation for P-waves in VTI media that depends on only two parameters, the NMO velocity  $V_{\text{nmo}}$  and anellipticity coefficient  $\eta \equiv (\epsilon - \delta)/(1 + 2\delta)$ :

$$T^2(x) = T_0^2 + \frac{x^2}{V_{\text{nmo}}^2} - \frac{2\eta x^4}{V_{\text{nmo}}^2 [T_0^2 V_{\text{nmo}}^2 + (1 + 2\eta) x^2]}. \quad (7)$$

Equation 7 is widely used in seismic processing to correct long-spread data for nonhyperbolic moveout and estimate the key anisotropy parameter  $\eta$ . The 3D version of the Alkhalifah-Tsvankin equation provides a close approximation to wide-azimuth P-wave traveltimes in orthorhombic or HTI media (Vasconcelos and Tsvankin, 2006):

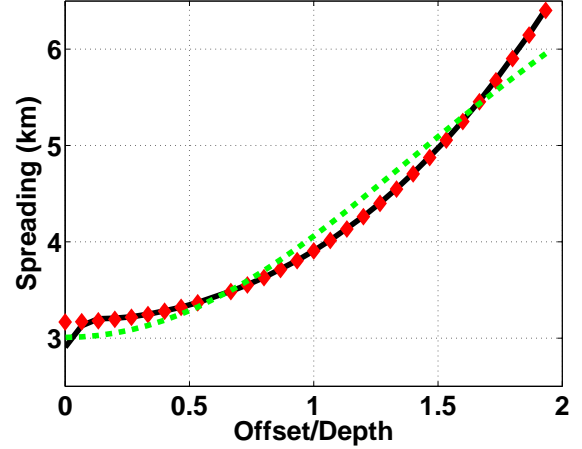


**Figure 3.** Geometrical spreading of PSV-waves reflected from the bottom of the VTI layer in model 1 (Table 1). Our method was applied with the Tsvankin-Thomsen equation 3 (diamonds) and with the Alkhalifah-Tsvankin equation 7 (dashed line); the solid line is computed by dynamic ray-tracing code ANRAY (Gajewski and Pšenčík, 1987).

$$T^2(x, \alpha) = T_0^2 + \frac{x^2}{V_{\text{nmo}}^2(\alpha)} - \frac{2\eta(\alpha) x^4}{V_{\text{nmo}}^2(\alpha) [T_0^2 V_{\text{nmo}}^2(\alpha) + (1 + 2\eta(\alpha)) x^2]}, \quad (8)$$

$$V_{\text{nmo}}^{-2}(\alpha) = \frac{\sin^2 \alpha}{(V_{\text{nmo}}^{(1)})^2} + \frac{\cos^2 \alpha}{(V_{\text{nmo}}^{(2)})^2}, \quad (9)$$

$$\eta(\alpha) = \eta^{(1)} \sin^2 \alpha + \eta^{(2)} \cos^2 \alpha - \eta^{(3)} \sin^2 \alpha \cos^2 \alpha. \quad (10)$$

Equation 9, which is equivalent to equation 5 discussed above, describes the NMO ellipse with the semi-axes  $V_{\text{nmo}}^{(1)}$  and  $V_{\text{nmo}}^{(2)}$ ;  $\eta^{(1,2,3)}$  are the anellipticity parameters in the three mutually orthogonal symmetry planes of the model. Xu and Tsvankin (2006a, 2006b) used equations 8–10 to compute the geometrical spreading of P-waves in horizontally layered, azimuthally anisotropic media.

Although equations 7 and 8 were originally designed for P-waves, it is worthwhile to test them for PS-waves. While we cannot expect the analytic form of the parameters  $V_{\text{nmo}}$  and  $\eta$  to be the same for P- and PS-waves, the geometrical-spreading correction operates with the best-fit moveout parameters obtained from semblance analysis. Therefore, we need to verify if the fit provided by equations 7 and 8 to converted-wave moveout is sufficient for accurate geometrical-spreading computation using MASC (equation 2).

First, we apply equations 3 and 7 to approximate the moveout of a PSV reflection from the bottom of a VTI layer sandwiched between two isotropic halfspaces (Figure 3 and Table 1). The best-fit moveout param-

	Layer 1	Layer 2	Layer 3
Symmetry type	ISO	VTI	ISO
Thickness (km)	0.5	1.0	$\infty$
Density (g/cm <sup>3</sup> )	2.0	2.1	2.2
$V_{P0}$ (km/s)	1.7	2.2	2.2
$V_{S0}$ (km/s)	0.8	1.1	1.0
$\epsilon$	0	0.23	0
$\delta$	0	0.10	0
$\gamma$	0	0.10	0
$\eta$	0	0.10	0
$\sigma$	0	0.64	0

**Table 1.** Parameters of a medium that includes a VTI layer sandwiched between two isotropic layers (model 1). The velocities and anisotropy parameters of the VTI layer are taken from the measurements for Dog Creek shale listed in Thomsen (1986).

	Layer 1	Layer 2	Layer 3
Symmetry type	VTI	ORTH	ISO
Thickness (km)	0.5	1.0	$\infty$
Density (g/cm <sup>3</sup> )	2.1	2.1	2.2
$V_{P0}$ (km/s)	2.2	2.2	2.2
$V_{S0}$ (km/s)	1.1	1.1	1.0
$\epsilon^{(1)}$	0.23	0.317	0
$\delta^{(1)}$	0.10	-0.054	0
$\gamma^{(1)}$	0.10	0.513	0
$\epsilon^{(2)}$	0.23	0.121	0
$\delta^{(2)}$	0.10	0.046	0
$\gamma^{(2)}$	0.10	0.138	0
$\delta^{(3)}$	0	0.1	0
$\eta^{(1)}$	0.1	0.42	0
$\eta^{(2)}$	0.1	0.07	0
$\eta^{(3)}$	0	0.05	0
$\sigma^{(1)}$	0.64	1.48	0
$\sigma^{(2)}$	0.64	0.31	0

**Table 2.** Parameters of a medium composed of VTI, orthorhombic, and isotropic layers (model 2). Orthorhombic symmetry can be described by the two vertical velocities ( $V_{P0}$  for P-waves and  $V_{S0}$  for one of the split S-waves) and seven anisotropy parameters ( $\epsilon^{(1)}$ ,  $\epsilon^{(2)}$ ,  $\delta^{(1)}$ ,  $\delta^{(2)}$ ,  $\delta^{(3)}$ ,  $\gamma^{(1)}$ , and  $\gamma^{(2)}$ ); the parameter values are based on the measurements of Wang (2002). The anellipticity parameters  $\eta^{(1)}$ ,  $\eta^{(2)}$ ,  $\eta^{(3)}$  control P-wave nonhyperbolic moveout, while  $\sigma^{(1)}$  and  $\sigma^{(2)}$  are largely responsible for the moveout of SV-waves in the vertical symmetry planes. For a detailed explanation of the notation, see Tsvankin (2005).

ters are then substituted into the geometrical-spreading equation 2. In agreement with the results of Tsvankin (2005), equation 3 provides an excellent approximation for PSV-wave moveout and yields a geometrical-spreading factor that is almost identical to that computed by dynamic ray tracing (Figure 3). Although the performance of the Alkhalifah-Tsvankin equation 7 is somewhat inferior, it has the advantage of being con-

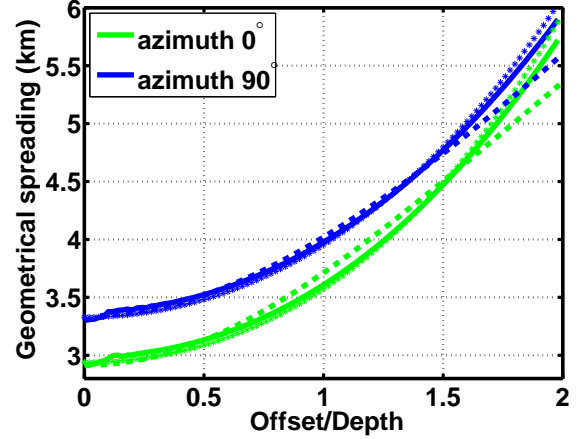


**Figure 4.** Geometrical spreading of PSV-waves reflected from the bottom of the orthorhombic layer in model 2 (Table 2). The azimuths  $\alpha = 0^\circ$  and  $\alpha = 90^\circ$  correspond to the symmetry planes  $[x_1, x_3]$  and  $[x_2, x_3]$ , respectively. Our method was applied with the 3D Tsvankin-Thomsen equation 4 (stars) and with the 3D Alkhalifah-Tsvankin equation 8 (dashed lines); the solid lines are computed by dynamic ray tracing.

sistent with the P-wave formalism while still providing adequate accuracy. It should be mentioned that the best-fit parameter  $\eta$  for PSV-waves is different from its analytic definition [ $\eta \equiv (\epsilon - \delta)/(1 + 2\delta)$  in a single VTI layer] for P-waves.

Next, the moveout approximations and the methodology of MASC are tested for the two vertical symmetry planes of orthorhombic media (Figure 4 and Table 2). Note that P-waves are coupled to two different split S-waves in the symmetry planes  $[x_1, x_3]$  and  $[x_2, x_3]$  (Tsvankin, 2005). Indeed, if the fast shear wave  $S_1$  is polarized in the  $x_1$ -direction at vertical incidence, it represents the SV mode that will produce P-to-SV conversion in the  $[x_1, x_3]$ -plane. Then the slow shear wave  $S_2$  will be responsible for the converted PSV-wave in the  $[x_2, x_3]$ -plane.

Since the symmetry planes of orthorhombic models are kinematically equivalent to VTI media, the travel-time fit provided by the moveout approximations in the incidence plane is the same as in VTI media. Geometrical spreading in azimuthally anisotropic media (equation 2), however, also depends on azimuthal traveltime variations away from the incidence plane (Tsvankin, 2005; Xu et al., 2005). Therefore, the accuracy of our method depends on the performance of the 3D versions of the moveout equations in the vicinity of the symmetry planes. As was the case for VTI media, the error of our method with the 3D Tsvankin-Thomsen equation 4 is almost negligible, while the 3D Alkhalifah-Tsvankin equation 8 produces some deviations from the ray-tracing result, especially at far offsets (Figure 4). Still, given relatively a large uncertainty in amplitude

measurements, the accuracy of equation 8 should be acceptable for purposes of AVO analysis.

### 3 APPLICATION TO AVO ANALYSIS OF SYNTHETIC DATA

In addition to potential problems with moveout approximations, the accuracy of amplitude corrections for mode conversions may be influenced by several other factors. Here, we do not consider PS-wave amplitudes in the anomalous areas near shear-wave cusps (triplications) and singularities, where AVO analysis is not practical. Still, the high sensitivity of S-waves to the presence of anisotropy may lead to rapid amplitude variations along PS wavefronts that are not adequately described by ray theory and, therefore, by MASC (Tsvankin, 2005). Also, even for models with a horizontal symmetry plane, the asymmetry of the PS raypath (i.e., the difference between the P- and S-legs) can result in a significant angular variation of transmission loss and related errors in AVO analysis. Hence, it is essential to test the performance of MASC for PS-waves on 3D full-wavefield synthetic data, as was done by Xu and Tsvankin (2006b) for P-waves.

The main question to be answered in this section is how accurately MASC can reconstruct plane-wave conversion coefficients in layered anisotropic media. An important practical issue is whether or not MASC can be replaced by empirical gain corrections in qualitative AVO analysis. Finally, we evaluate the magnitude of transmission loss (which is not included in MASC) and the related distortions of the PS-wave AVO response.

Due to the difficulties in modeling exact PS-wave amplitudes for layered orthorhombic media, we carried out amplitude processing only for the VTI medium from Table 1 (model 1). Synthetic seismograms were computed with the reflectivity code (ANISYNPA), which generates exact 3D wavefields for horizontally layered anisotropic media (e.g., Fryer and Frazer, 1984). A shot gather of the vertical displacement from a vertical force for model 1 is shown in Figure 5. The processing sequence is similar to that for P-waves described by Xu and Tsvankin (2006b). First, we apply the nonhyperbolic moveout equation 3 to the PS reflection from the bottom of the VTI layer to estimate the parameters  $A_2$ ,  $A_4$ , and  $A$ , which serve as the input to the geometrical-spreading correction. Second, the raw amplitudes are picked along the traveltime curve defined by equation 3 with the best-fit parameters. Third, MASC (equation 2) is applied to correct the picked amplitudes for anisotropic geometrical spreading. Fourth, the source and receiver directivity factors are removed using the local horizontal slowness.

To calibrate the P-wave AVO response, we matched the corrected amplitude at normal incidence with the exact reflection coefficient (Xu and Tsvankin, 2006b). This approach is not suitable for PS-waves because the

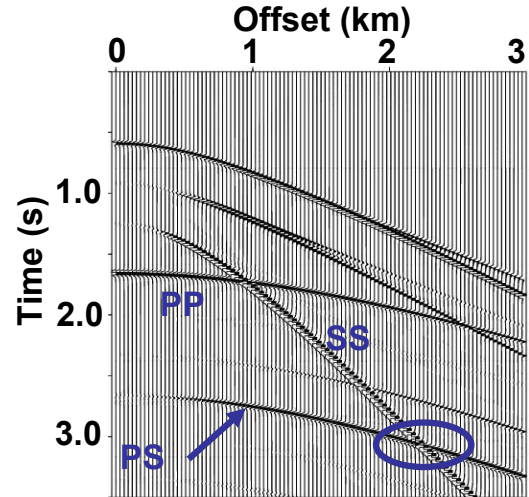


**Figure 5.** Synthetic shot gather for model 1 (Table 1) computed by the anisotropic reflectivity method. The top layer is specified as a halfspace to eliminate the influence of the free surface. The arrow marks the target PS-wave converted at the bottom of the VTI layer. The ellipse highlights the area of interference between the target event and the SS reflection from the top of the VTI layer.

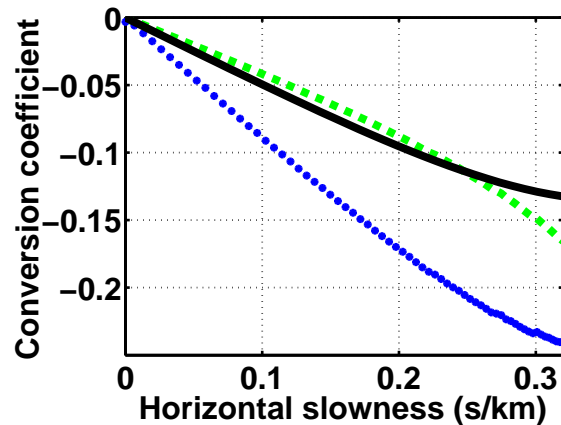


**Figure 6.** Conversion coefficient at the bottom of the VTI layer in model 1. The estimates obtained with MASC (dashed line) and the  $t$ -gain correction (dotted) are compared with the exact conversion coefficient (solid). The incidence angle of the downgoing P-wave corresponding to the maximum horizontal slowness (0.3 s/km) is  $30^\circ$ ; for the upgoing SV-wave, the corresponding angle is  $15^\circ$ .

conversion coefficient at normal incidence goes to zero. Since the source factor should be the same for both P- and PS-waves, we normalized the PS conversion coefficient using the scaling factor estimated for the corresponding P-wave reflection.

The high accuracy of MASC with the Tsvankin-Thomsen moveout equation for the model in Figure 5 was confirmed by the test in the previous section (see

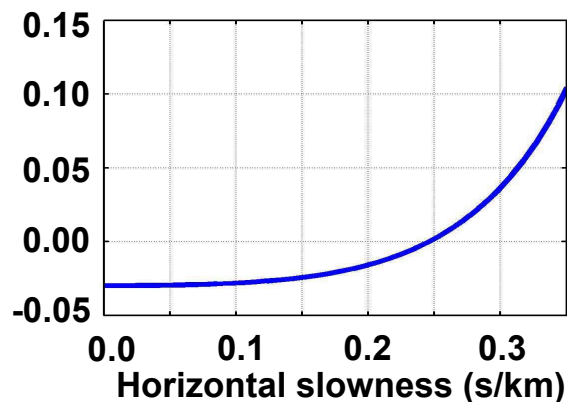


**Figure 7.** Transmission loss for the target PS-wave from Figure 5. The loss is computed by subtracting from unity the product of the plane-wave transmission coefficients along the raypath.

Figure 3). Still, the VTI layer has a significant value of the parameter  $\sigma$ , which is primarily responsible for SV-wave velocity anisotropy and angle-dependent geometrical spreading. Strong amplitude variations along the wavefront of the PS-wave may cause errors in the ray-theory equations employed in our method. Nevertheless, the conversion coefficient estimated by MASC is close to the exact values for a relatively wide range of horizontal slownesses (Figure 6).

In contrast, application of the conventional  $t$ -gain correction results in unacceptable errors even for small offsets. (The accuracy of the  $t^2$ -gain correction, not shown here, is lower.) Clearly, the influence of anisotropy significantly distorts geometrical spreading of PS-waves in typical TI models. Hence, AVO analysis for converted waves cannot be implemented without a robust anisotropic spreading correction.

The conversion coefficient reconstructed by MASC deviates from the exact values with increasing offset. This deviation is caused by the combined influence of the transmission loss and interference of the target PS event with the SS reflection from the top of the VTI layer (see the ellipse in Figure 5). Amplitude distortions caused by the interference with the SS-wave become especially severe for horizontal slownesses exceeding 0.3 s/km, which forced us to restrict the slowness range used in Figure 6.

The transmission coefficients for the upgoing and downgoing segments of reflected PP rays compensate for each other in such a way that their product (which determines transmission loss) is almost invariant with offset. For mode conversions, however, the upgoing and downgoing ray segments correspond to different modes, and this raypath asymmetry leads to an increase of the transmission loss for our model with offset (Figure 7). Since the geometrical-spreading correction does not account for transmission coefficients, this offset-dependent

transmission loss distorts the reconstructed conversion coefficient in Figure 6.

#### 4 DISCUSSION AND CONCLUSIONS

Geometrical spreading of shear and mode-converted waves typically is more strongly distorted by anisotropy than that of P-waves. Here, we showed that the moveout-based anisotropic spreading correction (MASC), previously developed for P-wave data, can be applied to PS-waves as well. For horizontally layered models, the geometrical-spreading factor of P- and PS-waves can be obtained from the same equation that involves traveltime derivatives with respect to offset and azimuth. This equation remains valid even for models without a horizontal symmetry plane, such as tilted transverse isotropy, in which reflection moveout of PS-waves becomes asymmetric (i.e., traveltime does not stay the same when the source and receiver are interchanged).

Because of the difficulty in dealing with split PS-waves in azimuthally anisotropic media, our implementation of MASC for mode conversions is restricted to VTI media and symmetry planes of orthorhombic and HTI media. To compute the traveltime derivatives required by MASC, we employed the Tsvankin-Thomsen nonhyperbolic moveout equation, which is used almost exclusively for P-waves. Still, numerical testing proves that this equation gives a close approximation for PSV-wave moveout both in layered VTI media and in the vicinity of the vertical symmetry planes of orthorhombic media. The three best-fit parameters of the Tsvankin-Thomsen equation serve as the input to the geometrical-spreading computation. Comparison with dynamic ray tracing shows that the accuracy of MASC for PS-waves is almost as high as for P-waves.

Furthermore, for purposes of geometrical-spreading correction PS-wave traveltimes can be adequately described by the simpler Alkhalifah-Tsvankin moveout equation. Whereas the analytic form of this equation is valid only for P-waves, it can be applied to mode conversions with fitted parameters  $V_{\text{nmo}}$  and  $\eta$ . The Alkhalifah-Tsvankin equation has the important advantage of making the MASC algorithm for PS-waves fully consistent with that for P-waves at the expense of somewhat lower quality of the traveltime fit.

Application of MASC to full-wavefield synthetic data from layered VTI media yields accurate estimates of the conversion coefficients for conventional-length spreads. The main complication in the reconstruction of conversion coefficients from surface data is related to offset-dependent transmission loss of PS-waves. The product of the transmission coefficients along the asymmetric raypath of mode conversions varies with incidence angle and, therefore, with offset. This variation, which is almost negligible for P-waves, is not accounted

for in the geometrical-spreading correction and can produce significant distortions of the AVO response at moderate and large offsets.

Our results demonstrate that even qualitative AVO analysis of PS-waves in the presence of anisotropy in the overburden requires application of the moveout-based anisotropic spreading correction. A promising direction for future studies is to extend MASC to split PS-waves outside of the symmetry planes of azimuthally anisotropic media. Such an extension is essential for developing robust azimuthal AVO algorithms operating with wide-azimuth mode-converted data.

## ACKNOWLEDGMENTS

We are grateful to members of the A(nisotropy)-Team of the Center for Wave Phenomena (CWP), Colorado School of Mines, for helpful discussions. The support for this work was provided by the Consortium Project on Seismic Inverse Methods for Complex Structures at CWP and by the Chemical Sciences, Geosciences and Biosciences Division, Office of Basic Energy Sciences, Office of Science, U.S. Department of Energy.

## REFERENCES

- Al-Dajani, A., I. Tsvankin, and M. N. Toksöz, 1998, Nonhyperbolic reflection moveout for azimuthally anisotropic media: 68th Annual International Meeting, SEG, Expanded Abstracts, 1479–1482.
- Alkhalifah, T., and I. Tsvankin, 1995, Velocity analysis for transversely isotropic media: *Geophysics*, **60**, 1550–1566.
- Bakulin, A., V. Grechka, and I. Tsvankin, 2000a, Estimation of fracture parameters from reflection seismic data – Part I: HTI model due to a single fracture set: *Geophysics*, **65**, 1788–1802.
- Bakulin, A., V. Grechka, and I. Tsvankin, 2000b, Estimation of fracture parameters from reflection seismic data – Part II: Fractured models with orthorhombic symmetry: *Geophysics*, **65**, 1803–1817.
- Červený, V., 2001, *Seismic ray theory*: Cambridge University Press.
- Dewangan, P., 2004, Processing and inversion of mode-converted waves using the PP+PS=SS method: Ph.D. thesis, Colorado School of Mines.
- Dewangan, P., I. Tsvankin, M. Batzle, K. van Wijk, and M. Haney, 2006, PS-wave moveout inversion for tilted TI media: A physical-modeling study: *Geophysics*, **71**, D135–D143.
- Fryer, G. J., and L. N. Frazer, 1984, Seismic waves in stratified anisotropic media: *Geophysical Journal of the Royal Astronomical Society*, **78**, 691–710.
- Gajewski, D., and I. Pšenčík, 1987, Computation of high frequency seismic wavefields in 3-D laterally inhomogeneous anisotropic media: *Geophysical Journal of the Royal Astronomical Society*, **91**, 383–412.
- Grechka, V., and I. Tsvankin, 1998, 3-D description of normal moveout in anisotropic inhomogeneous media: *Geophysics*, **63**, 1079–1092.
- Jilek, P., 2002, Modeling and inversion of converted-wave reflection coefficients in anisotropic media: A tool for quantitative AVO analysis: Ph.D. thesis, Colorado School of Mines.
- Neves, F. A., A. Al-Marzoug, J. J. Kim, and E. L. Nebrija, 2003, Fracture characterization of deep tight sands using azimuthal velocity and AVO seismic data in Saudi Arabia: *The Leading Edge*, **22**, 469–475.
- Rüger, A., 2001, Reflection coefficients and azimuthal AVO analysis in anisotropic media: Society of Exploration Geophysics.
- Rüger, A., and I. Tsvankin, 1997, Using AVO for fracture detection: Analytic basis and practical solutions: *The Leading Edge*, **16**, 1429–1434.
- Thomsen, L., 1986, Weak elastic anisotropy: *Geophysics*, **51**, 1954–1966.
- Thomsen, L., 1999, Converted-wave reflection seismology over inhomogeneous, anisotropic media: *Geophysics*, **64**, 678–690.
- Tsvankin, I., 1995, Body-wave radiation patterns and AVO in transversely isotropic media: *Geophysics*, **60**, 1409–1425.
- Tsvankin, I., 2005, *Seismic signatures and analysis of reflection data in anisotropic media*, 2nd ed.: Elsevier Science Publ. Co., Inc.
- Tsvankin, I., and V. Grechka, 2000, Dip moveout of converted waves and parameter estimation in transversely isotropic media: *Geophysical Prospecting*, **48**, 257–292.
- Tsvankin, I., and L. Thomsen, 1994, Nonhyperbolic reflection moveout in anisotropic media: *Geophysics*, **59**, 1290–1304.
- Vasconcelos, I., and I. Tsvankin, 2006, Non-hyperbolic moveout inversion of wide-azimuth P-wave data for orthorhombic media: *Geophysical Prospecting*, **54**, 535–552.
- Xu, X., I. Tsvankin, and A. Pech, 2005, Geometrical spreading of P-waves in horizontally layered, azimuthally anisotropic media: *Geophysics*, **70**, D43–D53.
- Xu, X., and I. Tsvankin, 2006a, Anisotropic geometrical-spreading correction for wide-azimuth P-wave reflections: *Geophysics*, **71**, D161–D170.
- Xu, X., and I. Tsvankin, 2006b, Azimuthal AVO analysis with anisotropic spreading correction: A synthetic study: *The Leading Edge*, **24**, 1336–1342.
- Xu, X., and I. Tsvankin, 2007, A case study of azimuthal AVO analysis with anisotropic spreading correction: CWP Research Report (this volume).
- Wang, Z., 2002, Seismic anisotropy in sedimentary rocks, part 2: Laboratory data: *Geophysics*, **67**, 1423–1440.